

## Supplementary Information

### **Self-reductive mesoporous CuO<sub>x</sub>/Fe/silicate nanocomposite as a highly active and stable catalyst for methanol reforming**

Chien-Cheng Li<sup>a</sup>, Yan-Wun Chen<sup>b</sup>, Ran-Jin Lin<sup>c</sup>, Ching-Chun Chang<sup>d</sup>, Kuei-Hsien Chen<sup>a,d</sup>, Hong-Ping Lin<sup>b,\*</sup> and Li-Chyong Chen<sup>a,\*</sup>

<sup>a</sup> Center for Condensed Matter Sciences, National Taiwan University, Taipei 10617, Taiwan.

<sup>b</sup> Department of Chemistry, National Cheng Kung University, Tainan 701, Taiwan  
<sup>c</sup> Sing-Fu consulting Co. Ltd., Ping-Dong 900, Taiwan

<sup>d</sup> Institute of Atomic and Molecular Sciences, Academia Sinica, Taipei 10617, Taiwan

## I. Experimental Details

### (a) Apparatus

The mesoporous ( $\text{CuO}_x$ -5 wt% Fe-silicate)-based catalysts were examined using a JOEL JEM-2100 field-emission transmission electron microscopy (FE-TEM) equipped with X-ray energy dispersive microanalysis (EDAX). X-ray diffraction (XRD) patterns were obtained using a Bruker D8 Advance diffractometer with  $\text{Cu k}_{\alpha}$  radiation ( $\lambda = 0.1542 \text{ nm}$ ) operated at 40 kV and 40 mA.  $\text{N}_2$  adsorption–desorption isotherms at 77 K were obtained by a Micromeritics ASAP 2010 apparatus. Before each measurement the sample was heated under vacuum at 150 °C for 2 h. Temperature programmed reduction (TPR) measurements were performed in a semiautomatic Micromeritics TPD/TPR 2920 apparatus fitted with a thermal conductivity detector (TCD) and interfaced to a microcomputer. X-ray photoelectron spectra (XPS) were obtained by a ULVAC-PHI PHI-Quantera SXM XPS system equipped the monochromatized  $\text{Al K } \alpha$  radiation (1486.6 eV). All binding energy (BE) values were calibrated using the C 1s peak at 284.6 eV as a reference.

### (b) Characterization of catalysts

The evaluation of the catalytic activity of the mesoporous ( $\text{CuO}_x$ -Fe-silica)-based catalysts was carried out by the oxidative steam reforming of methanol (OSRM) using a fixed-bed system under atmospheric pressure. A glass tube with an inner diameter of 3/8 inches was used as a reactor. For each experiment, approximately 150 mg of sample was packed between two quartz wool plugs to keep the catalyst bed in place. Mass loading of the film catalysts was held constant for all experiments in this study. The reactor tube was

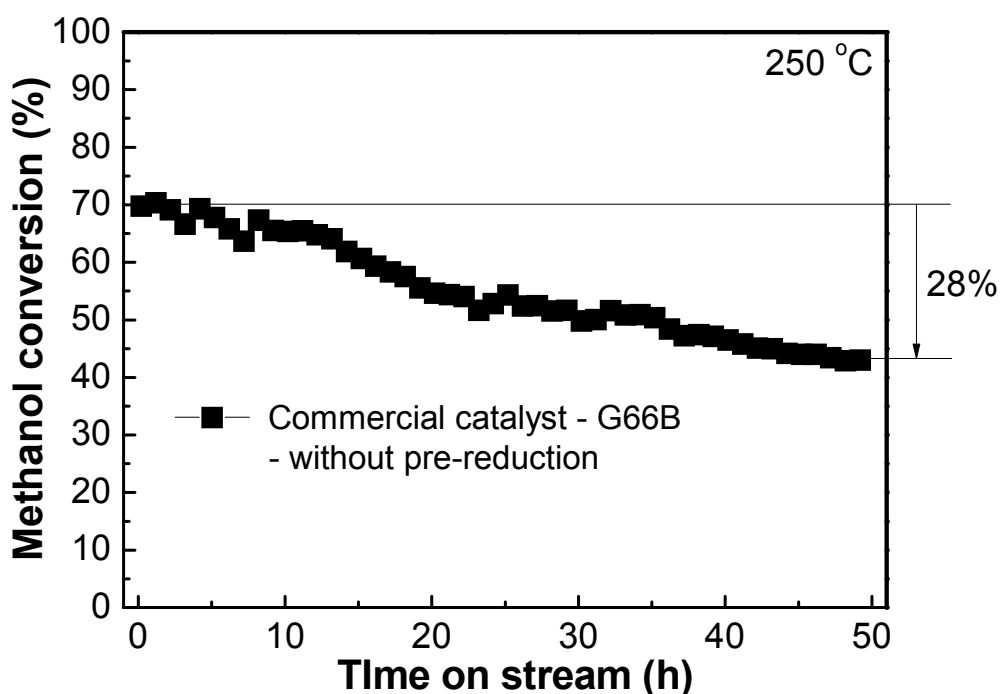
placed inside a horizontal tube furnace. A thermal couple was placed at the center of the catalyst bed. The OSRM tests were carried out in the temperature range of 150 °C – 300 °C and H<sub>2</sub>O/CH<sub>3</sub>OH/O<sub>2</sub> molar ratios of 1.25/1/0.25. The catalysts were pre-reduced at 300 °C for 1 h in a stream of 10% H<sub>2</sub>/N<sub>2</sub> mixture with a flow rate of 30 ml/min under the heating rate of 10 °C/min. The pre-mixed methanol and water solution was introduced by a syringe pump (KDS model 100). The liquids traveled a very short distance to an in-house built evaporator. The flow rate of the mixture of methanol and water was 1 ml/h. Gaseous feed (O<sub>2</sub>, N<sub>2</sub>) was regulated by an electronic mass flow controllers. The gas flows of N<sub>2</sub> and O<sub>2</sub> were 6.4 ml/min and 1.6 ml/min, respectively. Pipelines on the system were constructed of stainless steel tubes, which were wrapped by the heating tapes to avoid the condensation of the residual methanol and water in the pipelines. The composition of feed and product stream was analyzed by three on-line gas chromatographs in series (TCD-GC, China Chromatography CO., Ltd). Each injection through the GCs was 1 c.c., controlled by three automatic valves at a given time interval. The temperature of pipelines before the cooling system and the three valves was maintained between 110 °C and 130 °C in order to prevent any condensation of water.

## II. Results

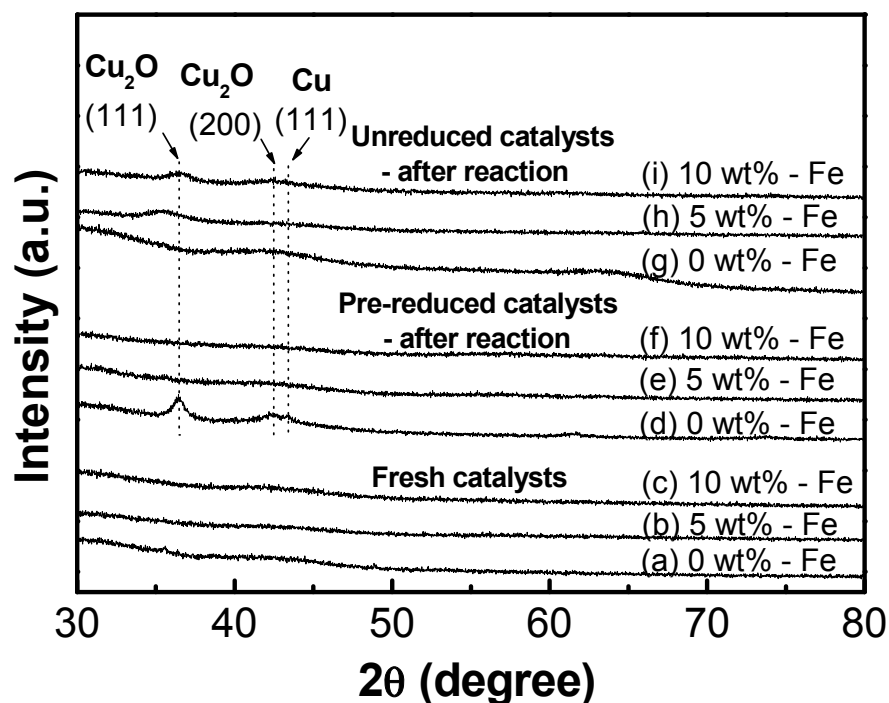
### 1. The X-ray diffraction patterns of the mesoporous ( $\text{CuO}_x$ -Fe-silicate)-based catalysts with and without pre-reduction for OSRM reactions at temperature of 250 °C after 50 h (or 12 h for ( $\text{CuO}_x$ -silicate)-based catalyst without pre-reduction) test.

Fig. S2 shows the XRD patterns of the mesoporous ( $\text{CuO}_x$ -Fe-silicate)-based catalysts with and without reduction treatments, and operating after the OSRM reactions at 250 °C for 50 h. No additional characteristics of crystalline  $\text{CuO}_x$  or  $\text{FeO}_x$  was observed in the diffraction patterns of the mesoporous ( $\text{CuO}_x$ -Fe-silicate)-based catalysts, as shown in Fig. S2 curves (a)–(c). In parallel to the TEM images and its electron diffraction pattern with diffuse pattern as shown in Fig. 1(a) and the inset of Fig. 1(a), respectively, the  $\text{CuO}_x$  and  $\text{FeO}_x$  in the mesoporous ( $\text{CuO}_x$ -5 wt% Fe-silicate)-based catalysts exhibit nanocrystallites. The absence of the high-angle XRD patterns indicates that the  $\text{CuO}_x$  and  $\text{FeO}_x$  species are highly dispersed in the silicate matrix. For the samples after reductive treatment and OSRM reactions at 250 °C for 50 h, no high-angle XRD diffraction peaks are found in the ( $\text{CuO}_x$ -Fe-silicate)-based catalysts even at higher Fe content (10 wt%), as shown in Fig. S2 curves (e) and (f). However, diffraction peaks of the Cu and  $\text{Cu}_2\text{O}$  phases are found in the mesoporous ( $\text{CuO}_x$ -silicate)-based catalyst (Fig. S2 curve (d)). The crystalline size calculated by using the Scherrer's equation of the  $\text{Cu}_2\text{O}$  phase ( $D_{111}$ ) is around 9.0 nm. It indicated that there is a severe sintering of  $\text{CuO}_x$  and crystallite growth in the mesoporous ( $\text{CuO}_x$ -silicate)-based catalyst during the reductive treatment and reforming reaction at high temperatures. While in the unreduced samples after OSRM reaction at 250 °C for 50 h, no obvious diffraction peaks are found

for the mesoporous ( $\text{CuO}_x\text{-Fe-silicate}$ )-based catalysts after OSRM reaction at 250 °C for 50 h (or 12 h for ( $\text{CuO}_x\text{-silicate}$ )-based catalyst), as shown in Fig S2 curves (g)–(i). Therefore, the presence of the well-dispersed  $\text{Cu}_2\text{O}$  and Cu metallic phase in the silicate matrix results in a high activity and stability of the ( $\text{CuO}_x\text{-Fe-silicate}$ )-based catalysts with and without reductive treatment. In comparison to the ( $\text{CuO}_x\text{-silicate}$ )-based catalyst, the absence of Fe leads to low activity and stability.



**Figure S1.** The time-dependent catalytic performance of the commercial catalyst (G66B) without pre-reduction for OSRM reaction at temperature of 250 °C after 50 h.



**Figure S2.** The X-ray diffraction patterns of the mesoporous ( $\text{CuO}_x$ -Fe-silicate)-based catalysts with and without pre-reduction for OSRM reactions at temperature of 250 °C after 50 h (or 12 h for ( $\text{CuO}_x$ -silicate)-based catalyst without pre-reduction) test.

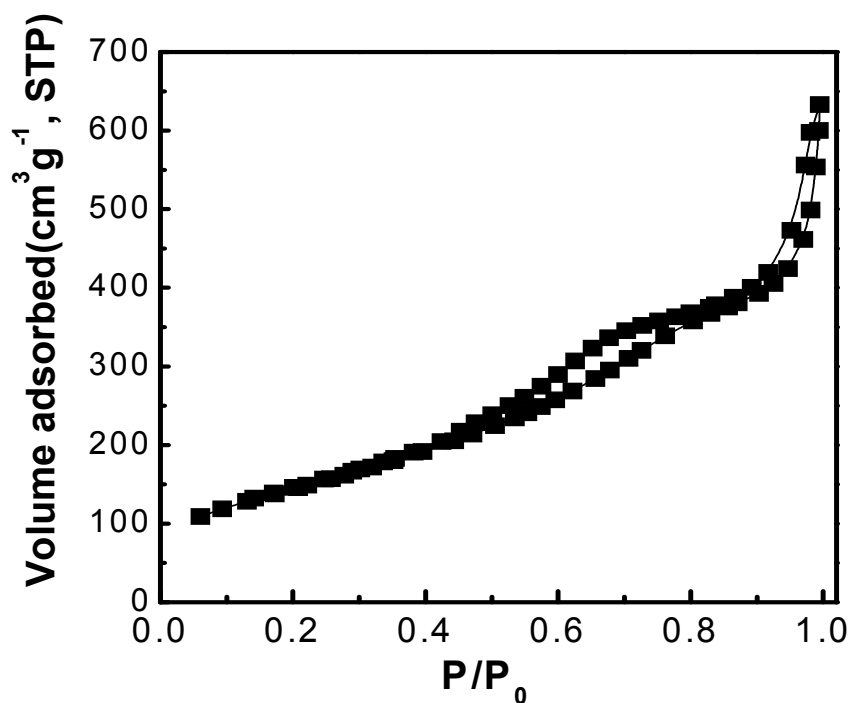


**Figure S3.** N<sub>2</sub> adsorption-desorption isotherm of the mesoporous (CuO<sub>x</sub>-5 wt% Fe-silicate)-based catalyst.

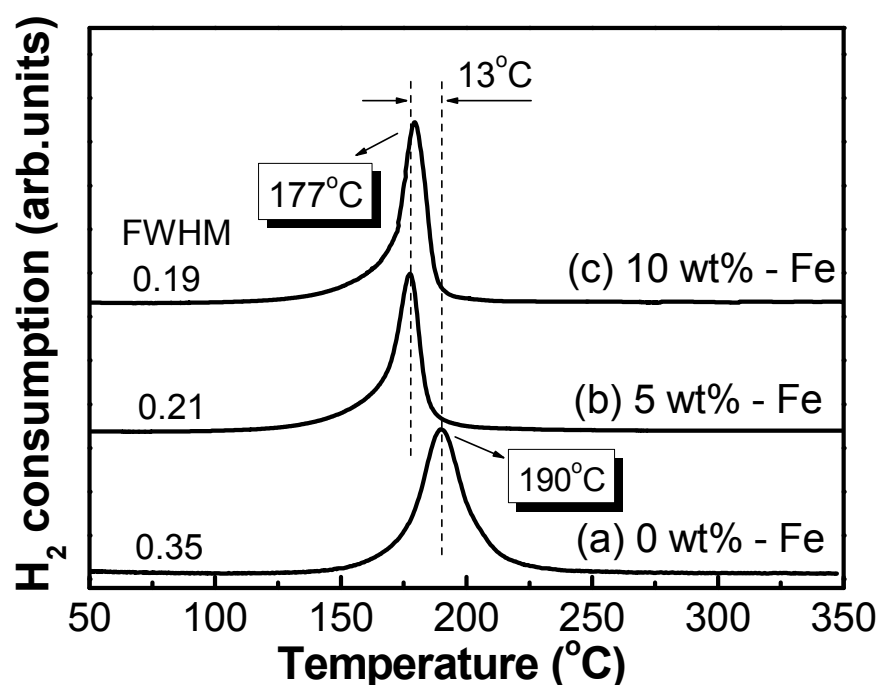


**Figure S4.** H<sub>2</sub>-TPR profiles of the mesoporous (CuO<sub>x</sub>-Fe-silicate)-based catalysts with various Cu/Fe ratios.

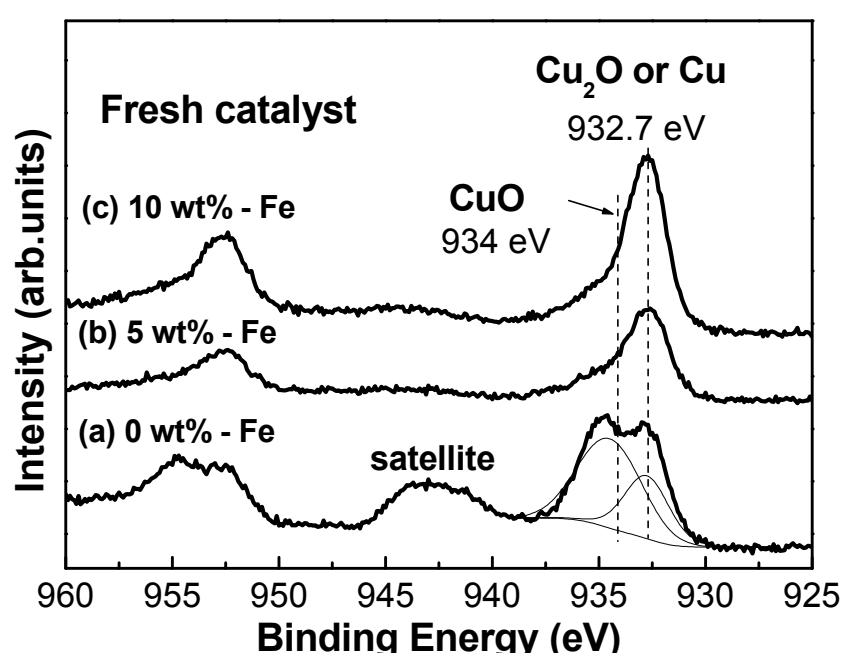


**Figure S5.** XPS spectra of the  $\text{Cu}$   $2p$  core level obtained from the  $(\text{CuO}_x\text{-Fe-silicate})$ -based catalysts with various  $\text{Cu}/\text{Fe}$  ratios.